# Plasma Boundary Effects at the Material Wall in Oblique Magnetic Fields

D. Curreli[1], R. Khaziev[1], A. Steinforth[1]

[1] *University of Illinois at Urbana Champaign, Urbana, IL 61801, USA*

## Abstract

We present a calculation of the ion energy distribution function (IEDF) and the ion angular distribution function (IADF) at the plasma-material interface in a magnetized plasma sheath, for magnetic fields inclined at an arbitrary angle with respect to the wall, and magnitudes up to one Tesla. As expected, the plasma sheath accelerates the ions up to energies scaled with the electron temperature. Surprisingly, the ion angular distributions exhibit non-linear trends.

## Introduction

At the boundary of a quasineutral magnetized plasma (Fig. 1), the magnetic pre-sheath and the thin electrostatic Debye sheath (DS) act as an interface between the bulk plasma and the material wall. The classical analysis done by Chodura [1] evidenced the structure of this transition layer, finding that within this region, the ions are accelerated toward the material wall by a potential drop that remains relatively insensitive to the magnetic field. The analysis was restricted to a perfectly absorbing wall. However, a material wall releases impurities into the plasma [2], [3], affecting the structure of the plasma sheath, and modifying the current and particle balances in the near-wall region. The physical response of the material wall is fairly sensitive to the ion energy and angular distribution functions at the time of impact.

In the present work we present a calculation of the ion energy distribution function (IEDF) and the ion angular distribution function (IADF) at the plasma-material interface of a magnetized plasma sheath. The magnetic field is inclined at a generic angle with respect to the normal to the wall. The ions accelerate, gyrate, and ExB-drift while passing through the sheath. In the next sections we summarize the results obtained using two different calculation techniques, namely (1) a semi-analytical Monte Carlo method, coupling a fluid model of the presheath (collisional + magnetic) to a particle-solver for the Debye Sheath, propagating the trajectories of a drifting Maxwellian population of ions across the ExB field of the free-charged layer, and (2) a three-dimensional kinetic-kinetic Particle-in-Cell.

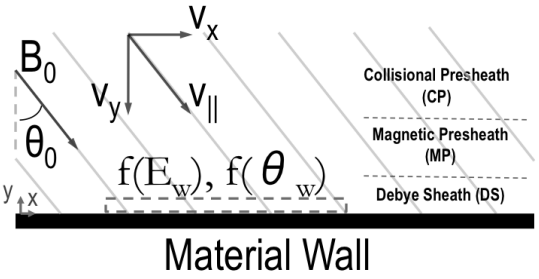


Figure 1: *Ion energy and angular distributions are calculated at the plasma-material interface with oblique B*

**Plasma Motion from the Presheath to the Wall**

In the classical unmagnetized case, an electrostatic Debye sheath is formed at the interface between a plasma and a solid surface. Ions enter the Debye sheath with a drift velocity equal to or greater than the ion acoustic velocity, $v_0 \geq C_s$ (Bohm criterion), and are supersonically accelerated by the sheath electric field. The addition of a magnetic field (B-field) changes the ion dynamics at the plasma-wall interface; Chodura [1] has shown that a quasi-neutral magnetic presheath appears when a magnetic field is inclined at an angle to the solid surface, changing the structure of the ordinary unmagnetized presheath. The ion drift velocity in direction parallel to the magnetic field at the entrance of the magnetic presheath has to be equal or greater than the ion acoustic velocity, $v_{||} \geq C_s$ (Chodura criterion).

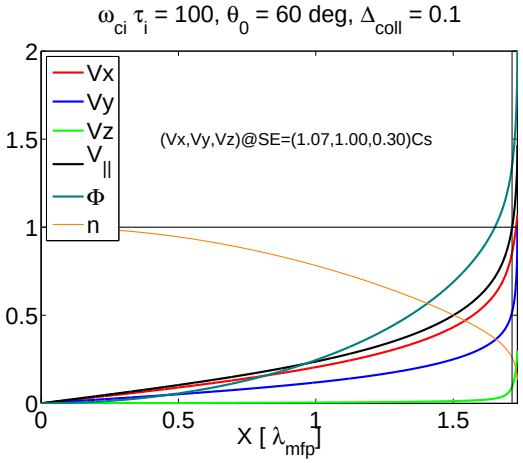


Figure 2: *Ion drift velocity ($V_x$,$V_y$,$V_z$,$V_{||}$) in the presheath; normalized potential & density*

Even if the size of the magnetic presheath changes at larger inclinations of the magnetic field, the total potential drop $\phi_0$ across the sheath remains relatively insensitive to the magnetic field, and for a floating wall it is equal to $-e\phi_0/KT_e = \log(1/2\pi \cdot M_i/m_e)^{1/2}$. The potential drop across the collisionless Chodura layer is $-e\phi_0/KT_e = \ln(\cos\theta_0)$, where $\theta_0$ is measured from the normal to the surface (Fig. 1), so that the resulting potential drop across the Debye sheath results $e\phi_0/KT_e = -\ln(\cos\theta_0) + \frac{1}{2}\ln(2\pi m_e/M_i)$. At high $\theta_0$ (grazing incidence) the total potential drop $\phi_0$ goes to zero, and above a critical angle $\theta_0^*$ the DS disappears.

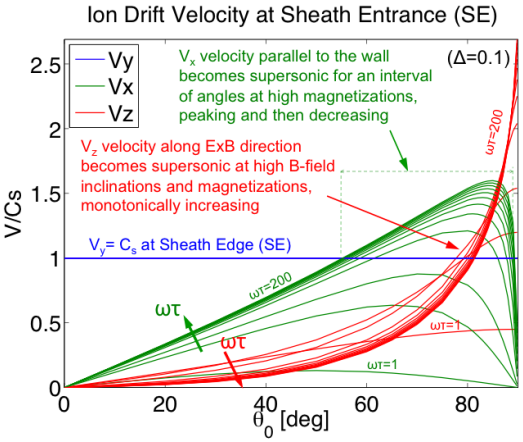


Figure 3: *Ion drift velocity at Sheath Entrance vs. the inclination $\theta_0$ of the magnetic field, at different levels of magnetization $\omega\tau$.*

The plasma flow in the collisional presheath (CP) and the magnetic presheath (MP) is solved using Riemann's hydrodynamic model of the magnetized presheath [4]-[5]. An example of calculation is reported in figure 2, for a strongly-magnetized weakly-collisional plasma ($\omega_{ci}\tau_i = 100$, with $\omega_{ci}$ ion cyclotron freq., $\tau_i$ ion collision time; $\theta_0 = 60$ deg; $\Delta_{coll} = 0.1$ ratio of the ionization and total collision frequency). The ion Mach number at the entrance of the electrostatic sheath (SE) is obtained for all three components of the velocity vector. Figure 3 shows the

components of the ion drift velocity as a function of the angle of inclination $\theta_0$ of the magnetic field. While crossing the CP and MP, the plasma accelerates and deviates with respect to the magnetic field direction, up to the entrance of the DS.

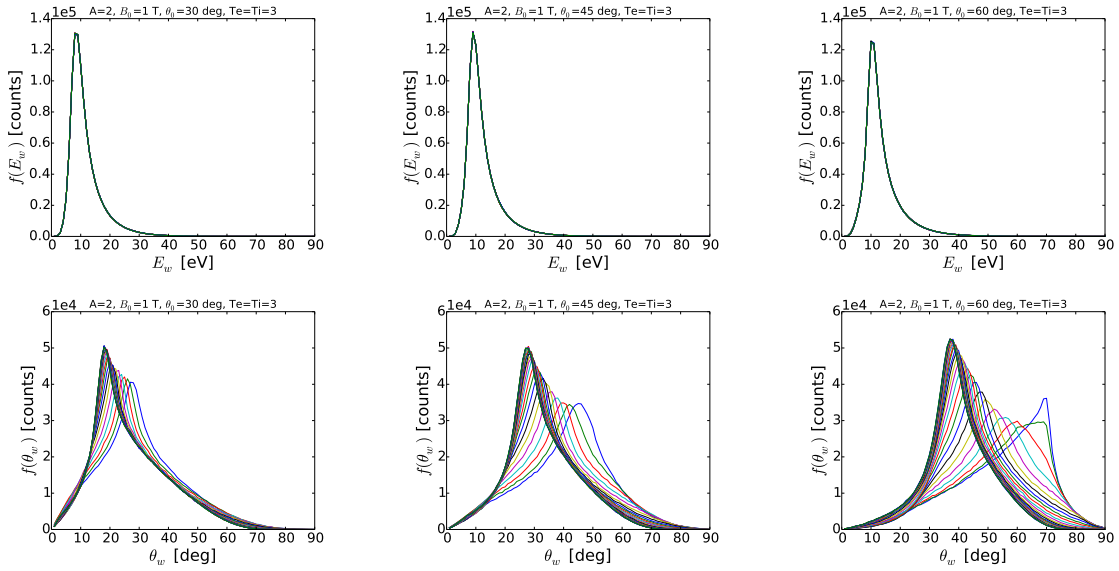


Figure 4: *(Top) Energy distribution functions, and (Bottom) angular distributions functions of deuterium ions at the material wall, at three inclinations of the B-field*

The strong electric field in the DS tends to reorient the plasma flow even further. Nevertheless, the ions never strike the wall at normal incidence. In the limit of weak collisionality, the trajectories of a drifting Maxwellian population of particles can be propagated across the ExB field of the magnetized free-charged layer using a Monte Carlo method up to the point where the ions hit the material wall.

**Ion Distributions at the Material Wall**

Figure 4 (Top) shows typical IEDF's for deuterium ions in a field $B_0 = 1$ Tesla inclined at $\theta_0 = 30, 45, 60$ degrees w.r.t the surface normal, calculated using the Monte Carlo method previously described. Each plot reports the distributions for densities in the range $n_e = 10^{16}$-$10^{20}$ m$^{-3}$ at 30 logarithmically-spaced points. The IEDF's at the wall remain independent than the density; a weak dependance upon the B-field angle $\theta_0$ is observed (of the order of a fraction of an eV), being due by the non-linear acceleration in the magnetic

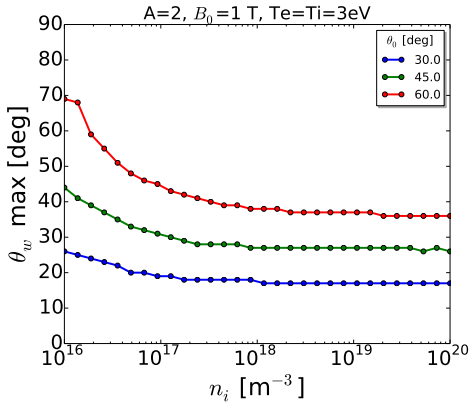


Figure 5: *Trend of the peak of the angular distribution at the wall vs. plasma density*

presheath.

Figure 4 (Bottom) reports the corresponding IADS's. A remarkable dependance upon the plasma density is observed. Figure 5 show the peaks of the angular distributions as a function of the density. The peak of the angular distribution occurs at angles $\theta_w$ smaller than the B-field inclination $\theta_0$. At lower densities the plasma impact on the wall at angles close to $\theta_0$. At higher densities an asymptotic behavior is observed, following approximately a rule $\theta_w^{max} \approx (2/3)\theta_0$.

The IEDF's and IADF's at the wall have been calculated also using a kinetic-kinetic Particle-in-Cell method. Figure 6 shows an example of results for $B_0 = 1.0$ T, $\theta_0 = 60$ deg, $T_e = 1.79$ eV, $n_e = 9 \times 10^{18}$ m$^{-3}$. Here the temperature and densities refer to the conditions once the plasma reaches stationary conditions. The distributions are obtained from the time averaged statistics (over one ion cyclotron period) of the particles crossing the boundary. Fig. 6.a shows the Electron Energy Distribution Function at the wall. As expected, the wall is reached by a Maxwellian electron flux corresponding to the electron temperature $T_e$. Fig. 6.b shows the IEDF, with the energy scale normalized to the average energy $\langle E \rangle = (1/2)M_i\langle v_i^2 \rangle$. The distribution is the sum of at least two ion populations: one drifting Maxwellian population scaled with the electron temperature, and one broader population at lower energy. The IADF at the wall (Fig. 6.c) peaks at around 40 degrees, in agreement with the MC predictions. However, the full-width half maximum of the PiC distributions is smaller than the one obtained from the MC model. As expected, the MC model neglects collective effects that the PiC takes consistently into account, the most important being: cooling consequent to supersonic ion acceleration, non-Boltzmann electron kinetics, finite-Larmor radius, plasma waves formation, and waves-sheath interaction.

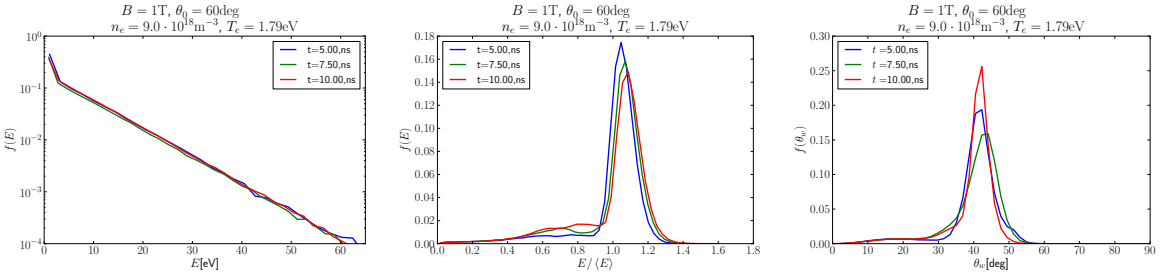


Figure 6: *(a) Electron Energy Distribution (b) Ion Energy Distribution, and (c) Ion Angular Distribution at the Material Wall, calculated using a kinetic-kinetic Particle-in-Cell method*

## References

[1] R. Chodura, Physics of Fluids, vol. 25, no. 9, pp. 1628-1633 (1982)
[2] Y. Yamamura and H. Tawara, Atomic Data and Nuclear Data Tables 62, 149-253 (1996)
[3] W. Moller and W. Eckstein, Nucl. Instr. and Meth. in Phys. Res.B 2, 814 (1984)
[4] K.U. Riemann et al., Phys. Plasmas 1, 552 (1994); Contrib. Plasma Phys. 34, 127 (1994)
[5] T. M. G. Zimmermann, M. Coppins, and J. E. Allen, Phys. Plasmas 15, 072301 (2008)